Bulletin of the College of Engineering, N.T.U., No. 92, October 2004, pp. 119–126
國立臺灣大學「台大工程」學刊　第九十二期　民國九十三年十月　第 119–126 頁

A MECHATRONICS APPROACH TO THE SERVO DESIGN FOR A MEGLEV SYSTEM

以機電整合為基礎之磁浮系統伺服設計

Jia-Yush Yen[*]　　*Jia-Hua Lin*[**]
顏家鈺　　林家豪

[*]Professor　[**]Graduate Student
Department of Mechanical Engineering, National Taiwan University, Taipei, Taiwan 10617, R.O.C.
[*]教授　[**]研究生
國立台灣大學機械工程學系

摘　要

所謂機電整合 (或說電子機械) 強調的是以智慧型的感應器與驅動器減低控制系統設計的複雜程度。文獻中有很多利子討論如何藉這項技術改善系統的性能。本文藉一高度非線性多自由度的磁浮系統爲載具 (一般均認爲需要先進的非線性控制才能成功者) 來展示以智慧型機械的方式從事設計的確有效果，但是如果設計的時候對於感應器與驅動器之間的關係沒有小心的處理，則其結果可能完全無法控制。因此良好的伺服設計必須對整體系統有一了解，配合系統的特性來安排驅動器與感應器之間的關係。從本研究的實驗結果顯示，機電整合之下的控制系統比複雜的非線性控制效果還要好。

關鍵詞： 機電整合、磁浮系統、主動剛性。

Abstract

The mechatronics approach emphasis the use of smart sensors and actuators to reduce the effort involved with complicated control system design. Many literatures reported the successful application of this approach, and people took for granted that smart sensors and actuators always helped to achieve better control performance. This paper uses the servo design of a highly nonlinear multi-degree-of-freedom Magnetic levitation (Maglev) system to illustrate that the mechatronics approach is, in fact, effective; however, a poor sensor-actuator configuration can also lead to design difficulty. It often requires more involved investigation to adequately assign the sensor-actuator relationship. The experimental results in this paper show that proper partitioning among the subsystems simplifies the control design, and the mechatronics approach achieves superior system performance.

Keywords: mechatronics, maglev suspension system, active stiffness.

1. INTRODUCTION

The mechatronics approach in servo design offers two advantages: better system performance and easier servo design. The mechatronics approach offers better performance because the vast amount of processors in the intelligent sensors and actuators can share the computation load. The processors only perform very simple control logics and they can sample at very high sampling rates. Fast sampling usually translates into higher servo bandwidth, and thus better performance. The mechatronics approach offers easier servo design because the central controller now only deals with many stable subsystems. The sensor and actuator subsystems are also easier to design because they only use less complicated algorithms.

There are many successful applications reported in the literature [1~10]. Basically, most of the results reported the design of various smart sensors and actuators. There is not really many reports concerning whether the mechatronics approach is more efficient. After all, there are rigorous mathematical proofs for the traditional controllers to show that they are stable, and the proofs always translate into systematic design

procedure. The mechatronics approach based on smart sensors and actuators, on the other hand, still lacks the kind of mathematical tools for the design. Of course, most of the systems using mechatronics approach are very complicate. It is hard to precisely describe it with a mathematical model anyway.

This paper would like to make a comparison between the traditional nonlinear control approach and the mechatronics approach. For this purpose, it is important to use a very complicate system such that simple control approach would not seem possible [11~18]. Because the maglev systems can vary in different configurations, the controller designs also have to vary accordingly [19~22]. As a result, these controllers are usually dependent on very precise mathematical models [23]. In this paper, a precision magnetic levitation (Maglev) stage is chosen as the target system. To realize the high precision requirement, the Maglev stage is equipped with sensors to detect five degree-of-freedom motion and actuators to maintain steady attitude. This paper first presents the design of a sophisticate nonlinear controller to meet the high precision servo specification. The nonlinear controller is based on the multivariable feedback linearization technique, and it is capable of incorporating linear high bandwidth specifications. Apparently, this approach is difficult to derive and it takes floating-point processor with a lot of computation power to implement.

Alternatively, a simple control with inherent mechatronics concept is attempted. It is possible to pair the sensors and actuators in the maglev system into single-input-single-output control loops. The PID controllers in each loop are tuned independently. It is shown that even though the sensors are reasonably paired with their neighboring actuators, the interference among different modes of platform motion resulted overall system does not maintain the performance expected.

By decomposing the system into approximate single-input single-output (SISO) linear subsystems, one can apply classical linear controllers to the subsystems. However, an experimental implementation reveals that an intuitive assignment of stable input-output pairs does not guarantee overall system stability. Instead, the coupling effects among the actuators completely messes-up the system behavior. With the help of the kinematic analysis, it is possible to come up with a subsystem division that minimizes the coupling effects. This new decomposition enables a straightforward tuning process. The experimental results are also in accordance with the design goal.

The following section will provide a brief description of the experimental maglev system. The system is designed to achieve long distance and high precision positioning. Section 3 will describe the mechatronics servo design concept and the decomposition of the subsystems. Section 4 will present the experiment results and compare the different subsystem decomposition. Section 5 will provide concluding remarks and some further research works.

2. REPULSIVE MAGLEV SYSTEM DESCRIPTION

Figure 1 shows the experimental maglev suspension system. Repulsive forces generated by the interaction between two groups of permanent magnets provide the essential lift force. These repulsive levitation forces cause the carriage to be laterally unstable. Separate devices called stabilizers (Fig. 2) are designed to stabilize this unstable carriage dynamics.

The stabilizers apply electromagnetic forces to the carriage magnets used for levitation. The carriage magnets, track magnets and stabilizers constitute the levitation tracks and there are four levitation tracks in the system. Figure. 3 shows the six degrees of freedom in the carriage dynamics, X, Y, Z, θ, ϕ and ψ, among which the θ and X degrees of freedom are unstable.

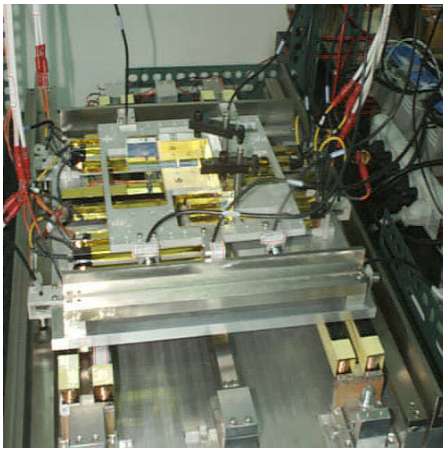

Fig. 1 Experimental magnetic levitation stage

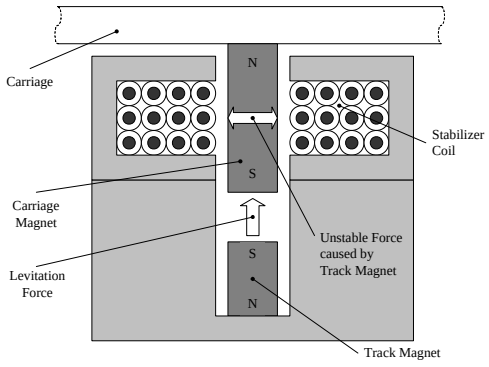

Fig. 2 The cross-section of the levitation track

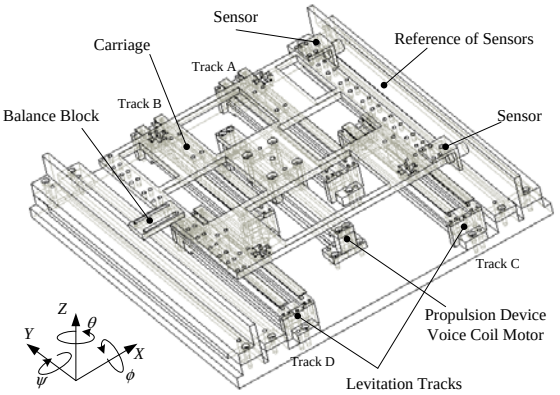

Fig. 3 A 3-D view of the maglev suspension system

The levitation and literal stabilizing coil generate the necessary control force to maintain the stage attitude. Accordingly, it is necessary to discuss the mechanical dynamics and the electrical dynamics.

2.1 Mechanical Dynamics

The mechanical dynamics for this maglev system was originally developed by Wang [8], and Huang derived a more complete nonlinear model in a control-affine form [13]:

$$\begin{aligned}\ddot{x}_1 &= f_1(x_1,x_2)+g_{11}(x_1,x_2)I_1+g_{12}(x_1,x_2)I_2\\ \ddot{x}_2 &= f_2(x_1,x_2)+g_{21}(x_1,x_2)I_1+g_{22}(x_1,x_2)I_2\end{aligned}, \quad (1)$$

where x_1 and x_2 are the system dynamic variables θ and X. I_1 and I_2 are the current flows in the coil of the electromagnets (stabilizers). f_1, f_2, g_{11}, g_{12}, g_{21}, g_{22} are nonlinear scalar functions of the form:

$$f_1(x_1,x_2)=\frac{I_M m_Z}{J}[2(-a_1+b_1x_1)\xi_1(x_1,x_2) +2(a_2+b_2x_1)\xi_2(x_1,x_2)], \quad (2)$$

$$f_2(x_1,x_2)=\frac{I_M m_Z}{M}[2\xi_1(x_1,x_2)+2\xi_2(x_1,x_2)], \quad (3)$$

$$g_{21}(x_1,x_2)=\frac{m_Z}{J}[2(-a_1+b_1x_1)\xi_3(x_1,x_2)], \quad (4)$$

$$g_{12}(x_1,x_2)=\frac{m_Z}{J}[2(a_2+b_2x_1)\xi_4(x_1,x_2)], \quad (5)$$

$$g_{21}(x_1,x_2)=\frac{m_Z}{M}[2\xi_3(x_1,x_2)], \quad (6)$$

$$g_{22}(x_1,x_2)=\frac{m_Z}{M}[2\xi_4(x_1,x_2)], \quad (7)$$

and

$$\xi_1(x_1,x_2)=\frac{\mu_0}{2\pi}\left\{\frac{[e_M^2-(c_M-a_1x_1+x_2)^2]}{[(c_M-a_1x_1+x_2)^2+e_M^2]^2}, +\frac{[e_M^2-(-c_M-a_1x_1+x_2)^2]}{[(-c_M-a_1x_1+x_2)^2+e_M^2]}\right\}$$

$$\xi_2(x_1,x_2)=\frac{\mu_0}{2\pi}\left\{-\frac{[e_M^2-(c_M+a_2x_1+x_2)^2]}{[(c_M+a_2x_1+x_2)^2+e_M^2]^2} +\frac{[e_M^2-(-c_M+a_2x_1+x_2)^2]}{[(-c_M+a_2x_1+x_2)^2+e_M^2]^2}\right\},$$

$$\xi_3(x_1,x_2)=\frac{\mu_0 N}{2\pi}\left\{\frac{-(d-a_1x_1+x_2)^2}{[(d-a_1x_1+x_2)^2]^2} +\frac{-(-d-a_1x_1+x_2)^2}{[(-d-a_1x_1+x_2)^2]^2}\right\},$$

$$\xi_4(x_1,x_2)=\frac{\mu_0 N}{2\pi}\left\{\frac{-(d+a_2x_1+x_2)^2}{[(d+a_2x_1+x_2)^2]^2} +\frac{-(-d+a_2x_1+x_2)^2}{[(-d+a_2x_1+x_2)^2]^2}\right\},$$

where a_1, a_2, b_1, b_2, c_M, d, e_M and N are dimensional parameters. μ_0, the permeability of free space, is a constant and equal to $4\pi \times 10^{-7}$H/m.

2.2 Electrical Dynamics

The electrical dynamics of the maglev suspension system can be treated as two independent inductance-resistance circuits as:

$$\dot{I}_1=-\frac{R_1}{L_1}I_1+\frac{K_{A1}}{L_1}u_1=\tau_{e1}I_1+K_{e1}u_1, \quad (8)$$

$$\dot{I}_2=-\frac{R_2}{L_2}I_2+\frac{K_{A2}}{L_2}U_2=\tau_{e2}I_2+K_{e2}u_2, \quad (9)$$

where R_1, R_2 are the resistors of the electromagnet coils, L_1, L_2 are the inductors of the electromagnet coils, and K_{A1}, K_{A2} are gains of the linear power amplifiers. u_1, u_2 are the control voltages to the amplifiers. They serves as the control input variables. The complete model then requires the combination of the mechanical and the electrical dynamics.

3. CONTROLLER DESIGN

The controller is proposed that will stabilize the

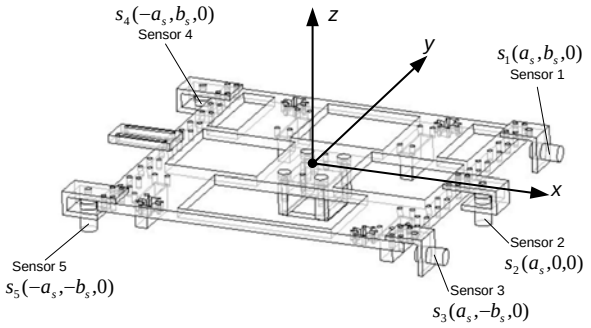

Fig. 4 Sensor configurations for the maglev system

system outputs, lateral translation (X) and rotation with respect to Z axis (θ), by two inputs, a control signal for inner tracks' stabilizers (u_1) and the outer tracks' stabilizers (u_2). The experimental maglev system composes of 5 induction-type proximity sensors to measure distances required to determine the control parameters (Fig. 4).

The range of the sensors are 0 ~ 2mm. The output of the sensor can be adjusted between 0~2 Volts, and the resolution of the sensor is 0.1% of the measurement range up to a frequency bandwidth of DC~3.3kHz (-3dB). In this experiment, the resolution is 2 μm. Using the Eular angle description, the relationship between a fixed coordinate X-Y-Z and the body coordinate x-y-z can be written as

$$\begin{bmatrix} X \\ Y \\ Z \end{bmatrix} = \mathbf{T} \cdot \begin{bmatrix} x \\ y \\ z \end{bmatrix} \tag{10}$$

where

$$\mathbf{T} = \begin{bmatrix} \cos\theta\cos\phi & -\sin\theta\cos\zeta + \cos\theta\sin\phi\sin\zeta & \sin\theta\sin\zeta + \cos\theta\sin\phi\cos\zeta \\ \sin\theta\cos\phi & \cos\theta\cos\zeta + \sin\theta\sin\phi\sin\zeta & -\cos\theta\sin\zeta + \sin\theta\sin\phi\cos\zeta \\ -\sin\phi & \cos\phi\sin\zeta & \cos\phi\cos\zeta \end{bmatrix}$$

is the transformation matrix. If the position of the sensors on the stage are

$$s_{1,\mathrm{xyz}} = \begin{bmatrix} s_{1,\mathrm{x}} \\ s_{1,\mathrm{y}} \\ s_{1,\mathrm{z}} \end{bmatrix} = \begin{bmatrix} a_\mathrm{s} \\ b_\mathrm{s} \\ 0 \end{bmatrix}, \quad s_{2,\mathrm{xyz}} = \begin{bmatrix} s_{2,\mathrm{x}} \\ s_{2,\mathrm{y}} \\ s_{2,\mathrm{z}} \end{bmatrix} = \begin{bmatrix} a_\mathrm{s} \\ 0 \\ 0 \end{bmatrix},$$

$$s_{3,\mathrm{xyz}} = \begin{bmatrix} s_{3,\mathrm{x}} \\ s_{3,\mathrm{y}} \\ s_{3,\mathrm{z}} \end{bmatrix} = \begin{bmatrix} a_\mathrm{s} \\ -b_\mathrm{s} \\ 0 \end{bmatrix}, \quad s_{4,\mathrm{xyz}} = \begin{bmatrix} s_{4,\mathrm{x}} \\ s_{4,\mathrm{y}} \\ s_{4,\mathrm{z}} \end{bmatrix} = \begin{bmatrix} -a_\mathrm{s} \\ b_\mathrm{s} \\ 0 \end{bmatrix},$$

$$s_{5,\mathrm{xyz}} = \begin{bmatrix} s_{5,\mathrm{x}} \\ s_{5,\mathrm{y}} \\ s_{5,\mathrm{z}} \end{bmatrix} = \begin{bmatrix} -a_\mathrm{s} \\ -b_\mathrm{s} \\ 0 \end{bmatrix} \tag{11}$$

where a_s, b_s are known dimensions. If one assume small pitch and yaw angle for the precision servo, the sensor position can be calculated as

$$s_{1,\mathrm{XYZ}} = \begin{bmatrix} s_{1,\mathrm{X}} \\ s_{1,\mathrm{Y}} \\ s_{1,\mathrm{Z}} \end{bmatrix} = \begin{bmatrix} a_\mathrm{s} - b_\mathrm{s}\theta + X \\ a_\mathrm{s}\theta + b_\mathrm{s} \\ -a_\mathrm{s}\phi + b_\mathrm{s}\zeta + Z \end{bmatrix},$$

$$s_{2,\mathrm{XYZ}} = \begin{bmatrix} s_{2,\mathrm{X}} \\ s_{2,\mathrm{Y}} \\ s_{2,\mathrm{Z}} \end{bmatrix} = \begin{bmatrix} a_\mathrm{s} + X \\ a_\mathrm{s}\theta \\ -a_\mathrm{s}\phi + Z \end{bmatrix},$$

$$s_{3,\mathrm{XYZ}} = \begin{bmatrix} s_{3,\mathrm{X}} \\ s_{3,\mathrm{Y}} \\ s_{3,\mathrm{Z}} \end{bmatrix} = \begin{bmatrix} a_\mathrm{s} + b_\mathrm{s}\theta + X \\ a_\mathrm{s}\theta - b_\mathrm{s} \\ -a_\mathrm{s}\phi - b_\mathrm{s}\zeta + Z \end{bmatrix},$$

$$s_{4,\mathrm{XYZ}} = \begin{bmatrix} s_{4,\mathrm{X}} \\ s_{4,\mathrm{Y}} \\ s_{4,\mathrm{Z}} \end{bmatrix} = \begin{bmatrix} -a_\mathrm{s} - b_\mathrm{s}\theta + X \\ -a_\mathrm{s}\theta + b_\mathrm{s} \\ a_\mathrm{s}\phi + b_\mathrm{s}\zeta + Z \end{bmatrix},$$

$$s_{5,\mathrm{XYZ}} = \begin{bmatrix} s_{5,\mathrm{X}} \\ s_{5,\mathrm{Y}} \\ s_{5,\mathrm{Z}} \end{bmatrix} = \begin{bmatrix} -a_\mathrm{s} + b_\mathrm{s}\theta + X \\ -a_\mathrm{s}\theta - b_\mathrm{s} \\ a_\mathrm{s}\phi - b_\mathrm{s}\zeta + Z \end{bmatrix} \tag{12}$$

The attitude of the stage can now be calculated by the five sensor measurements.

$$\mathbf{H} = \begin{bmatrix} h_1(\theta,\phi,\zeta,X,Z) \\ h_2(\theta,\phi,\zeta,X,Z) \\ h_3(\theta,\phi,\zeta,X,Z) \\ h_4(\theta,\phi,\zeta,X,Z) \\ h_5(\theta,\phi,\zeta,X,Z) \end{bmatrix} = \begin{bmatrix} s_{1,\mathrm{X}} - a_\mathrm{s} \\ s_{2,\mathrm{Z}} \\ s_{3,\mathrm{X}} - a_\mathrm{s} \\ s_{4,\mathrm{Z}} \\ s_{5,\mathrm{Z}} \end{bmatrix} = \begin{bmatrix} -b_\mathrm{s}\theta + X \\ -a_\mathrm{s}\phi + Z \\ b_\mathrm{s}\theta + X \\ a_\mathrm{s}\phi + b_\mathrm{s}\zeta + Z \\ a_\mathrm{s}\phi - b_\mathrm{s}\zeta + Z \end{bmatrix} \tag{13}$$

The carriage magnets in the system receive the forces from the magnetic tracks. There are four carriage magnets in Fig. 3 located among the centerline of the magnetic tracks. It is nature to decompose the input-output pairs by pairing the force-receiving magnet with the closest sensor. The five sensors thus derived five subsystems. As will be discussed later, this configuration resulted in a system that is very difficult to tune.

An alternate configuration thus arises from consideration of the system kinematics. The electric wires to the two inside rails are connected in series, thus they generate a force that lift up the front end of the carriage (Fig. 3). Likewise, the outside rails generate a force that lift up the rear end of the carriage. Two pair of the side forces can be treated similarly to move the front and rear end of the carriage in the x direction. The difference in the two pairs of side forces generates a torque that controls the yaw motion.

A hybrid controller that combines the bang-bang control for near saturation control in conjunction with a high performance pole-placement controller then serves as the servo controller. The controller parameters are tuned by assuming a linear system for experimental system identification. Notice that the system model is experimentally determined therefore the control parameter should achieve the desired control if the subsystem configuration is reasonable.

4. EXPERIMENTAL SETUP

The maglev suspension system considered is an electrically and mechanically integrated system (Fig. 5). The maglev suspension system consists of the mechanism, a set of power amplifiers as actuators, a Pentium 233 PC as the controller, inductive gauging sensors as feedback sources, a 12-bit ADC and a 12-bit DAC as system input-output devices. The resolution of sensors is 4μm and the bandwidth of sensors is 3.3 kHz. The control inputs are limited within ±9Volts to protect the stabilization coils. Due to the computational power of Pentium 233 PC, high-speed sampling is possible when complex control algorithm is implemented and because the calculation for the controller is very straight, the sampling frequency for the five axes can be as high as 2.5 KHz.

5. EXPERIMENTAL RESULTS AND DISCUSSION

The goals set for the maglev suspension system are a demonstration of stability, decoupling of the degrees-of-freedom, improving the system's rigidity. The result from the proposed first partition is shown in Figs. 6 and 7. Due to the space limit, only the more critical responses are included. Figure 6 shows the computed closed-loop frequency response from the experimentally identified subsystem from exciting the first pair of literal stabilizing coil to the first sensor output. The closed-loop bandwidth is 66 Hz. Figure 7 shows the step response of the same subsystem. Very good performance is observed.

Figures 8 and 9 shows the frequency and step responses for the sensor 3 subsystem. The step response looks poor and the closed-loop bandwidth is calculated to be 2.7 Hz. Both subsystem for sensor 3 and 4 shows particular low bandwidth. Increasing the loop gain by adjusting the controller parameters resulted in oscillatory responses. This is a result of improper subsystem partition. The system is stable when separately tuned, but when all the subsystem loops are activated, the side forces generated by the sensor 3 subsystem input coil also generate strong coupling effect to the other subsystems. Therefore, increasing loop gain affect the stabilizing action in the other control loops.

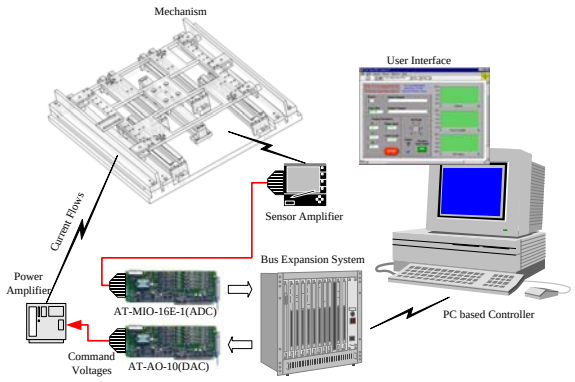

Fig. 5 The configuration of the repulsive maglev suspension system

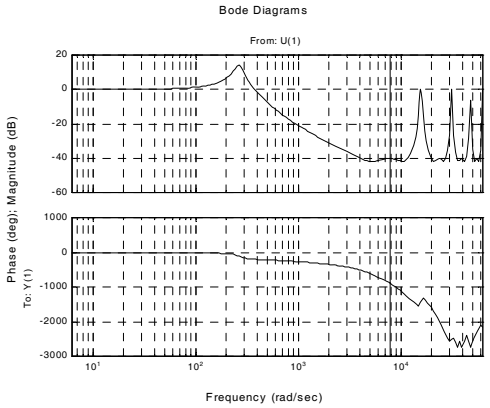

Fig. 6 Frequency response for the sensor 1 subsystem

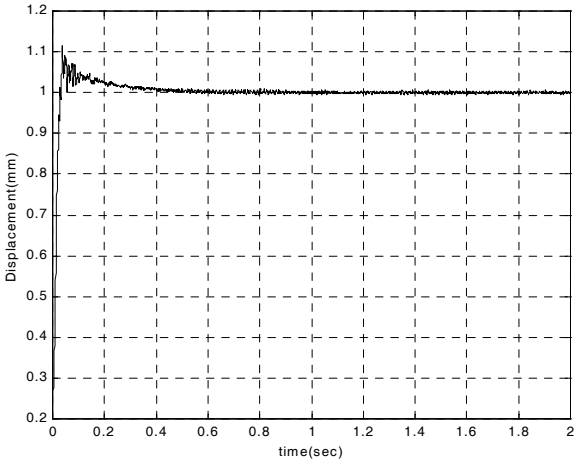

Fig. 7 Step response for the sensor 1 subsystem

As an attempt to correct this effect, the new subsystem partitioning is carried out. Figure 10 shows the closed-loop frequency response for the literal motion, and Fig. 11 shows the step response to the same subsystem.

The rest of the subsystems achieve similar performances. The bandwidths for the subsystems when all the loops are activated are consistently 53.15 Hz, 50.93 Hz, 46.95 Hz, 53.63 Hz, and 41.38 Hz. We see that the coupling effect is successfully suppressed and the overall system perform in consistent with the separate subsystem.

6. CONCLUSIONS

In this paper, a mechatronics approach to simplify the servo design for the maglev system is proposed. The mechatronics approach basically divided the complicated system into multiple local loops that may be separately controlled. The break up of the system enables the use of simple SISO control loops for the subsystems. This also lifted the limitation on the sampling rate derived from the complex controller computation. However, this paper also pointed out that careless assignment of the sensor/actuator pairs could lead to very hard to tune overall systems. The worse case can even cause system instability. A kinematics analysis provided in the paper leads to reasonable subsystem partitions, and overall system behavior that is consistent with the separate subsystem performance is achieved.

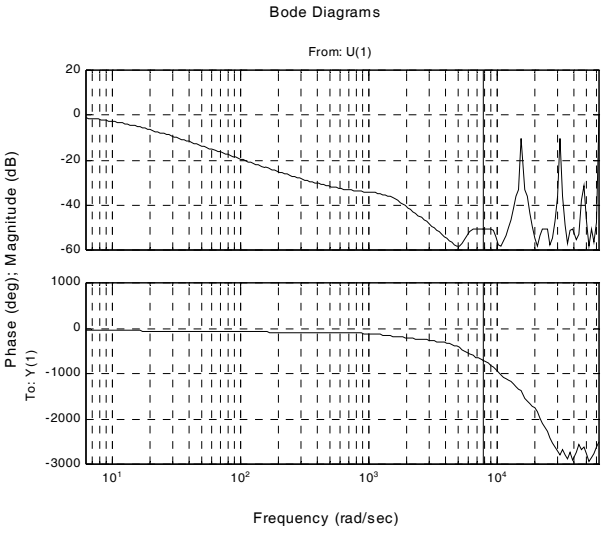

Fig. 8 Frequency response for the sensor 3 subsystem

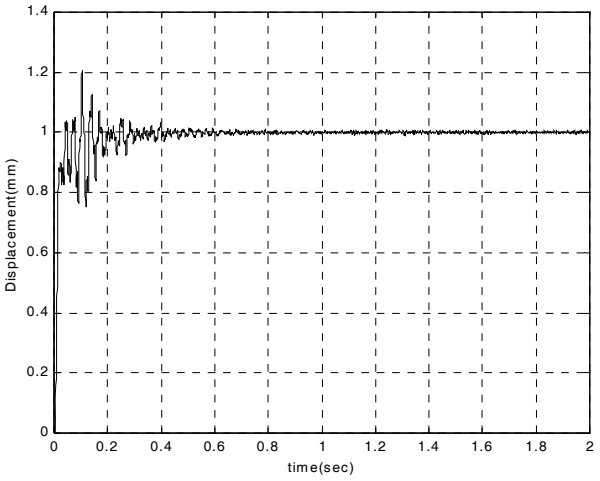

Fig. 9 Step response for the sensor 3 subsystem

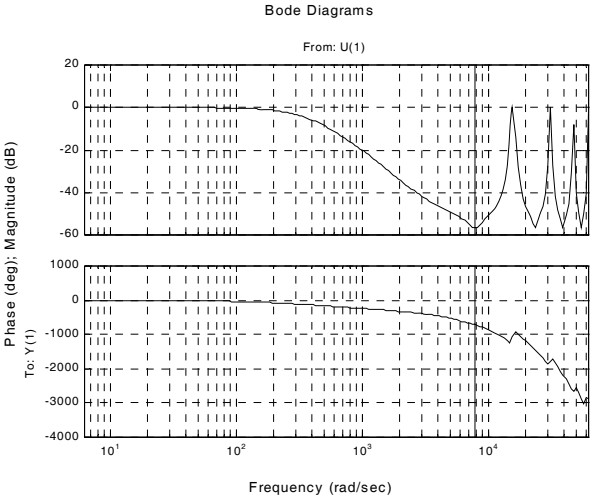

Fig. 10 Literal subsystem frequency response

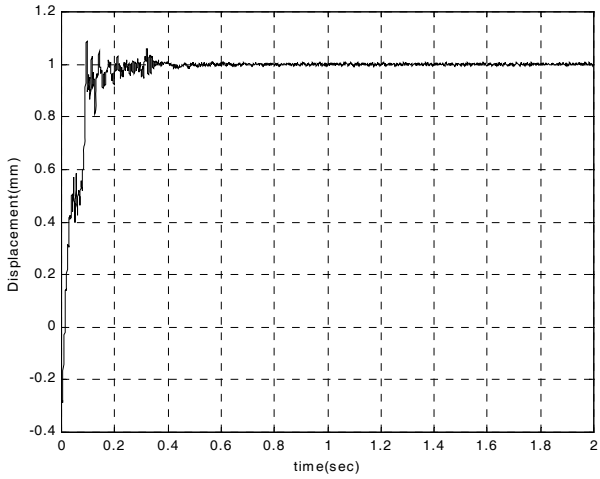

Fig. 11 Literal subsystem step response

ACKNOWLEDGEMENTS

This work is supported by the National Science Council, Taiwan R.O.C. under project No. NSC88-2213-E-002-083.

REFERENCES

[1] J. H. Zou, Z. L. Jing, M. Nakamura and A. Luo, "The modeling of mechatronic servo systems and vibration control," *American Society of Mechanical Engineers, Design Engineering Division*, Vol. 111, 2001, pp 17−21.

[2] A. Fulford and A. Alleyne, "An embedded mechatronic system for wireless servo control," *Proceedings of the American Control Conference*, Vol. 2, 2002, pp. 1658−1659.

[3] Y. Su, B. Duan, R. Nan and B. Peng, "Mechatronics design of stiffness enhancement of direct-drive motor systems using ER variable damper," *Chinese Journal of Mechanical Engineering*, Vol. 37, No. 8, 2001, pp. 78−79.

[4] M. G. Simoes and S. Szafir, "A DSP computer platform for mechatronics teaching and research," *Computers in Education Journal*, Vol. 13, No. 4, Oct./Dec. 2003, pp. 15−25.

[5] Y. Sato and C. H. Gakkai Ronbunshu, "Robust fuzzy neural network based control for mechatronic servo systems with high nonlinearity," *Transactions of the Japan Society of Mechanical Engineers*, Part C, Vol. 69, No. 11, Nov. 2003, pp 2929−2936.

[6] B. A. Hussein, "On modelling mechatronics systems—A geometrical approach," *Mechatronics*, Vol. 10, No. 3, 2000, pp. 307−337.

[7] Y. Su, B. Duan, R. Nan and B. Peng, "Mechatronics design of stiffness enhancement of direct-drive motor systems using ER variable damper," *Chinese Journal of Mechanical Engineering*, Vol. 37, No. 8, Aug. 2001, pp. 75−79.

[8] T. W. Tee, K. H. Low, H. Y. Ng and F. Young, "Mechatronics design and gait implementation of a quadruped legged robot," *Proceedings of the 7th International Conference on Control, Automation, Robotics and Vision*, ICARCV 2002, 2002, pp. 826−832.

[9] R. Horowitz, Y. Li and S. Park, "Mechatronics of electrostatic microactuators and micro-gyroscopes," *International Workshop on Advanced Motion Control*, AMC, 2000, pp. xxxi-xxxviii.

[10] J. Wagner, I. Paradis, E. Marotta and D. Dawson, "Enhanced automotive engine cooling systems — A mechatronics approach," *International Journal of Vehicle Design*, Vol. 28, No. 1-3, 2002, pp. 214−240.

[11] P. K. Sinha, Electromagnetic Suspension, *Dynamics and Control*, London. Peter Peregrinus, 1987.

[12] D. Cho, Y. Kato and D. Spilman, "Sliding mode and classical control of magnetic levitation systems," *IEEE Control Syst. Mag.*, Vol. 13, No. 1, 1993, pp. 42−48.

[13] D. L. Atherton, "Maglev using paermagnets," *IEEE Trans. Magn.*, Vol. 16, No. 1, 1980, pp. 146−148.

[14] M. Morishita, T. Azukizawa, S. Kanda, N. Tamura and T. Yokoyama, "A new maglev system for magnetically levitated carrier system," *1986 Int. Conf. Maglev and Linear Drives*, Vancouver, B. C., May 1986.

[15] O. Tsukamoto, K. Yasuda and J. Z. Chen, "A new magnetic levitation system with AC magnets," *IEEE Trans. Magn.*, Vol. 24, No. 2, 1988, pp. 1497−1500.

[16] R. Williams, J. R. Matey, Y. Arie and J. Rathee, "The effect of mass and pole strength on the levitation height of the magnet over a superconductor," *J. App. Phys.*, Vol. 65, No. 9, 1989, pp. 3583−3585.

[17] K. N. Wu and L. L. Chen, "Adaptive control of a four-track maglev system," *Journal of Control Systems and Technology*, Vol. 4, No. 4, 1996, pp. 295−302.

[18] I. Y. Wang, "A magnetic levitation silicon wafer transport system," Ph.D. Dissertation, The University of Texas at Austin, 1993.

[19] J. Huang, J. Y. Yen and M. S. Chen, "Adaptive nonlinear control of repulsive maglev suspension systems," *Control Engineering Practice*, Vol. 8, No. 12, Dec. 2000, pp. 1357−1367.

[20] O. Tsukamoto, K. Yasuda and J. Z. Chen, "A new magnetic levitation system with AC magnets," *IEEE Transactions on Magnetics*, Vol. 24, No. 2, 1988, pp. 1497−1500.

[21] R. Williams, J. R. Matey, Y. Arie and J. Rathee, "The effect of mass and pole strength on the levitation height of the magnet over a superconductor," *Journal of Applied Physics*, Vol. 65, No. 9, 1989, pp. 3583−3585.

[22] K. N. Wu and L. C. Fu, "Adaptive control of a four-track maglev system," *Journal of Control Systems and Technology*, Vol. 4, No. 4, 1996, pp. 295−302.

[23] C. M. Huang, "Nonlinear controller design of repulsive maglev suspension guiding system," Ph.D. Dissertation, The National Taiwan University, 1999.

Jia-Yush Yen (顏 家 鈺) 顏家鈺是一九八〇年國立清華大學動力機械系畢業，一九八三年美國明尼蘇達大學機械系碩士，一九八八年美國加州大學柏克萊分校控制系統博士。他畢業後即直接回到國立台灣大學機械系教書，其中曾爲工研院光電所顧問、機械所特約研究人員，亦曾擔任台北市捷運木柵線體檢委員，後來並擔任多次台北捷運初勘委員與交通部捷運旅勘委員，他並是ASME、IEEE、中國工程師學會、中國機械工程師學會、自動控制學會會員。

Jia-Hua Lin (林 家 豪) 林家豪出生於民國六十四年，台中縣立烏日國小、私立明道高中、台灣大學機械工程系畢業，他也是台灣大學機械系碩士，本論文是他在碩士時的工作，他目前是聯發科技公司的高級工程師。

收稿日期 93 年 2 月 5 日、修訂日期 93 年 8 月 20 日、接受日期 93 年 8 月 20 日
Manuscript received February 5, 2004, revised August 20, 2004, accepted August 20, 2004